PHYSICAL REVIEW B **71**, 241404(R) (2005)

Surface potential of a polar oxide film: FeO on Pt(111)

Emile D. L. Rienks, Niklas Nilius, Hans-Peter Rust, and Hans-Joachim Freund
Fritz-Haber-Institut der Max-Planck-Gesellschaft, Faradayweg 4-6, 14195 Berlin, Germany
(Received 31 March 2005; revised manuscript received 9 May 2005; published 8 June 2005)

We have studied a thin FeO film on Pt(111) using scanning tunneling microscopy. The corrugation of the Moiré pattern, that arises due to a lattice mismatch between the oxide film and the substrate, is found to increase dramatically when the microscope is operated in the field-emission regime. This contrast enhancement can be attributed to variations in the energy at which field-emission resonances are observed. We assign this effect to variations of the surface potential within the Moiré unit cell. Using a simple electrostatic model we show that in this oxide film with polar termination, such variations can be induced by very subtle differences in geometry.

DOI: 10.1103/PhysRevB.71.241404 PACS number(s): 73.30.+y, 68.47.Gh, 68.37.Ef

The distinct properties of polar oxide surfaces have stimulated intensive experimental and theoretical investigations.[1–5] The polarity arises from the stacking of atomic layers with an opposite net charge along the surface normal. In a perfect oxide, the dipole moment associated with each bilayer adds to the electrostatic surface energy, causing this quantity to diverge with increasing oxide thickness. Several mechanisms have been predicted by model calculations to compensate the oxide polarity. Among these are reconstruction of the surface layer, partial filling of surface states, and molecular adsorption.[2,4,5] A detailed understanding of these compensation mechanisms is desirable, because oxides with polar terminations are often characterized by a higher chemical reactivity and better wetting behavior with respect to their nonpolar counterparts.

In this work, we use an ultrathin FeO film grown on Pt(111) as a simple model system to study surfaces with a polar termination. Since Vurens *et al.* prepared the 1-ML-thick FeO film on Pt(111) (Ref. 6), many properties of this system have been resolved: It was found that the FeO thin film has a bilayer structure, which means that the surface has a polar termination. The oxygen atoms form the outermost layer in this structure, and the iron and oxygen planes are separated over 0.68 Å (Ref. 7). Laterally, the FeO layer is expanded with respect to the (111) layers in bulk FeO. The Fe nearest-neighbor distance is 3.1 Å in the film versus 3.0 Å in bulk FeO. The mismatch of this Fe—Fe distance with the nearest-neighbor distance of 2.76 Å in the Pt substrate gives rise to a Moiré pattern with a periodicity of about 25 Å. Due to this fairly large size of the unit cell, it has not been possible to apply quantitative diffraction or first-principles theoretical methods. As a consequence, a detailed structural model of the film is not available and a simplified structure has been used in theoretical treatments instead.[8,9]

It is, however, important to realize that regions with fairly distinct geometries can be identified in the unit cell. There are regions where Fe atoms occupy fcc and hcp hollow, as well as atop sites on the platinum substrate. It is therefore not unlikely that the film is rather inhomogeneous. In this paper we show that at least one property, the surface potential, varies within the Moiré unit cell. In addition, we show that scanning tunneling microscopy (STM) can be very sensitive to variations of this property.

The measurements described in this paper were performed with a scanning tunneling microscope operated in ultrahigh vacuum and at low temperature (5 K) (Ref. 10). Images are acquired in constant current mode, with a feedback set point of 0.3 nA. The FeO film is prepared by deposition of 1 ML of Fe onto a Pt(111) surface at room temperature and subsequent oxidation in 10^{-6} mbar O_2 at a temperature of 1000 K (Ref. 11).

As reported previously by various groups, a Moiré pattern appears in STM images of the thin FeO film.[8,11] The corrugation of this superstructure amounts to about 0.3 Å at bias voltages below 1 V, as can be seen in Fig. 1(a). Interestingly, we find a dramatic increase in the corrugation of the Moiré pattern if the sample bias voltage V_s is increased to 4500 mV. Height differences of up to 2 Å can be observed [Fig. 1(b)]. This is surprising because, generally, the corrugation decreases exponentially with increasing tip–sample distance.[12]

The bias voltage at which this dramatic enhancement in contrast is observed suggests that it is related to field-emission resonances.[13,14] These arise when the bias voltage exceeds the tip or sample work function, causing part of the tunneling gap to become classically accessible. The wave

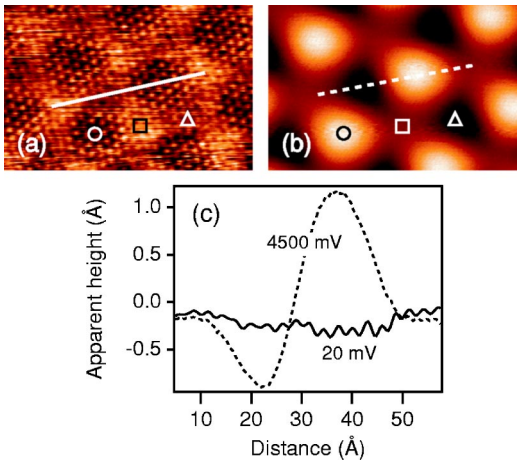

FIG. 1. (Color online) 75×50 Å^2 STM images at sample bias voltages of (a) 20 mV and (b) 4500 mV. (c) Line profiles from the STM images across the Moiré unit cell. $I_t=0.3$ nA.

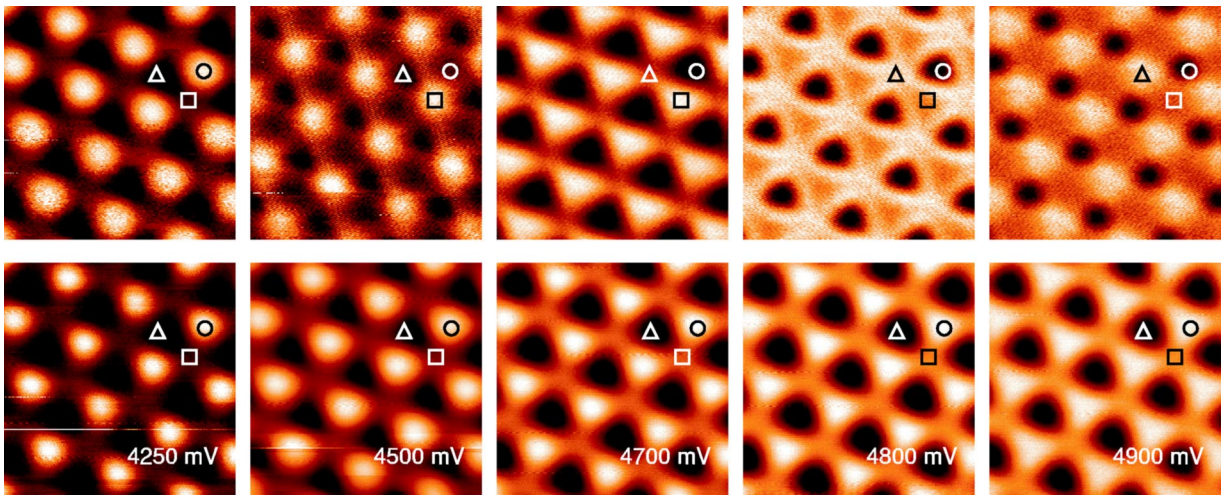

FIG. 2. (Color online) dI/dV (top) and topographic images. Image size 88×88 Å^2, $I_t=0.3$ nA.

function of an electron in this region is the sum of the forward tunneling wave and that reflected from the surface of the positive electrode. When this wave function matches the barrier shape, a standing wave is formed in the classically accessible region of the tip–sample gap, and the transfer probability is greatly enhanced.

We suggest that the strong contrast within the Moiré unit cell at bias voltages between 4200 and 5000 mV is a consequence of differences in the voltage at which the first field-emission resonance occurs. Topography and dI/dV images at various bias voltages in this range are given in Fig. 2. The conductance increase is first observed in those regions labeled with the circle. This explains the maxima in both topography and dI/dV images at 4250 mV. Subsequently, the field-emission resonance condition is fulfilled in those regions labeled with the square, as can be concluded from the dI/dV images taken at bias voltages in the range of 4500–4700 mV. As the topography images reflect the integrated conductance, the change in contrast in these images is less pronounced. Finally, the regions labeled with the triangle show the highest intensity in dI/dV images at bias voltages above 4800 mV.

The energy dependence of the transmission probability over a broader range can be seen in Fig. 3, where dI/dV spectra taken at the three different positions in the Moiré unit cell are shown. These spectra are recorded with a closed feedback loop to allow a large energy range to be covered in a single spectrum. The spectra display the same pattern as seen in the dI/dV images over the range from 4 to 5 V. In this range, the highest conductance is first observed at the position labeled with the circle, then at that labeled with the square, and finally at that with the triangle. It can also be seen in Fig. 3 that this pattern recurs for the second- and higher-order field-emission resonances, i.e., all field-emission resonances are observed with the lowest bias when the tip is above the position labeled with the circle. Finally, it is interesting to note that the peaks in spectra obtained at the "square" and "triangle" locations are split and have two, respectively, three maxima. We suggest that this splitting is due to fulfillment of the resonance condition between the tip and those neighboring regions of the sample where the resonance condition is fulfilled at lower bias. As a consequence, the spectrum taken at the location labeled with the circle is not split, because here the resonances occur at the lowest bias. From the splitting of the spectra it can be concluded that a sample area with a radius of at least 15 Å contributes to the current in these experiments. In spite of that value, the images in Fig. 2 show that the STM operated at these bias voltages is able to resolve features on a substantially smaller lateral scale.

In summary, we have seen that a strong contrast appears on the FeO surface when the STM is operated in the field-emission regime. This contrast can be attributed to local variations in the energy at which the first field-emission resonance occurs. What underlies this effect?

The energy at which field-emission resonances occur depends strongly on the surface potential.[15] Local variations in the surface potential can thus give rise to the observed in-

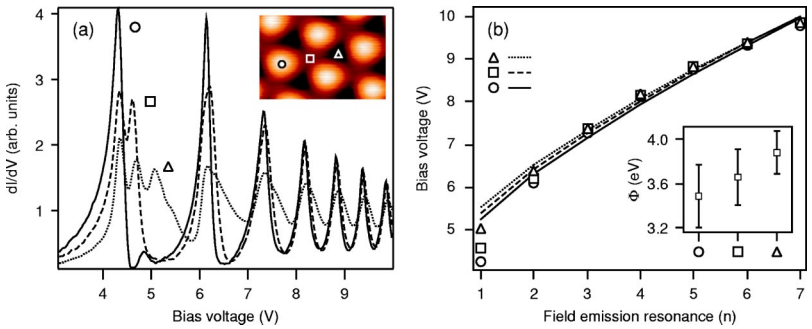

FIG. 3. (Color online) (a) dI/dV spectra obtained with closed feedback loop, taken at the three positions on the FeO film indicated in the inset (left). (b) Energies at which field-emission resonances are observed. The lines represent fits to the points with Eq. (1); first-order field-emission resonance have not been included in the fit. The inset shows the resulting values for the barrier Φ.

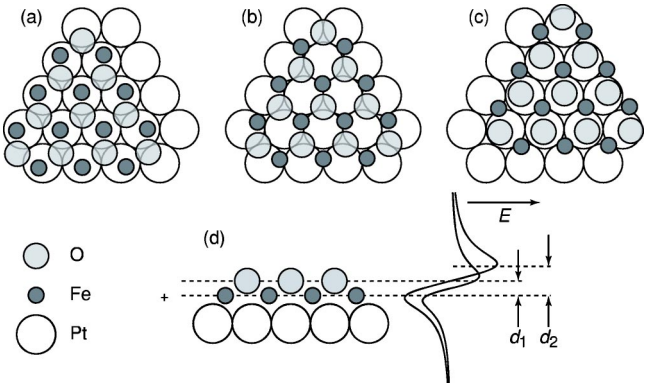

FIG. 4. Hard sphere models of the (a) top, (b) fcc, and (c) hcp regions in the FeO over-layer. Side view is sketched in (d) along with the electric field due to the polar bilayer for two different Fe-O separations, d_1 and d_2.

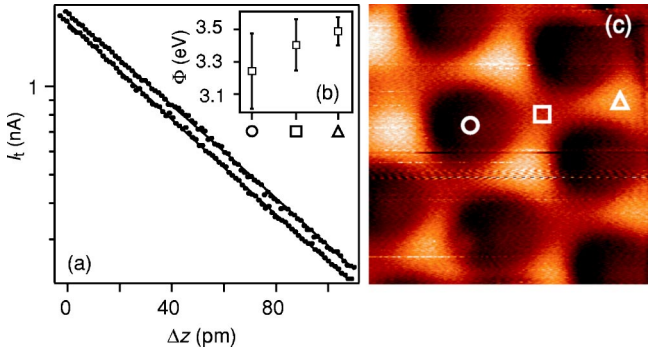

FIG. 5. (Color online) (a) Tunneling current vs tip-sample separation recorded at the two most distinct locations in the FeO unit cell. The solid lines represent fits to Eq. (2). (b) Resulting values for the barrier Φ, and (c) $d\ln I/dz$ image. Image size 57×57 Å^2, $V_s=4500$ mV, $I_t=0.3$ nA, $\Delta z_{\mathrm{rms}}=1$ Å.

crease in contrast. Alternatively, it is possible that the field-emission resonance merely amplifies local differences in the conductance due to other channels. For example, at a position with a relatively high state density, the tip-sample separation will increase to maintain a constant tunneling current. As a consequence, at this location the geometric resonance condition for the first field-emission mode is fulfilled at relatively low bias. In other words, conductance maxima are likely to induce field-emission resonances. However, this does not seem to be the case because we see that not only the first-, but also the higher-order field-emission resonances appear first at a particular position on the film. This would require that the conductance is highest here over a very large energy range of about 6 V. This makes the first explanation, that of variations in the surface potential, more appropriate.

What could cause such variations in the surface potential? It was mentioned above that the surface has a polar termination, which means that the Fe-O dipole contributes substantially to the surface potential. As a consequence, the potential will be affected by local variations of the Fe-O dipole strength. Such variations are to be expected, because of the inhomogeneous structure of the FeO thin film. Regions can be identified within the Moiré unit cell, where the Fe and O atoms assume very different positions with respect to the Pt substrate. These are sketched in Fig. 4. One can imagine that the distance d between the Fe and O planes will differ for the various regions. On the basis of the simple hard-sphere models given in Fig. 4, one would expect d to be smallest when the Fe atoms sit on top of Pt atoms and the oxygens are above threefold hollow sites [Fig. 4(a)]. The other extremum would be expected for the structure with Fe in hcp sites (c), and the intermediate case would be that where both Fe and O are above hollow sites (b).[18]

Assuming that $d_{\mathrm{top}}<d_{\mathrm{fcc}}<d_{\mathrm{hcp}}$, we obtain the following assignment of structural regions to the various positions in the STM images shown in Figs. 1 and 2: The top region [Fig. 4(a)] corresponds to the position labeled with the circle, fcc (b) with the square, and hcp with the triangle. Previously, Galloway *et al.* presented an interpretation of low-bias voltage STM images based on electron-scattering quantum chemistry calculations.[8] They have found that the top domains have the lowest apparent height but largest atomic corrugation. That is in agreement with the results we obtain at low bias [area labeled with the circle in Fig. 1(a)]. Galloway *et al.* however, assign the areas with largest apparent height at low bias (squares) to hcp regions. Here, the field-emission resonance is observed at intermediate voltage. Therefore, according to our model these would be fcc regions instead. It is important to stress that our assignment is tentative, as it relies on rather crude assumptions about how d will differ for the various geometries. A more sophisticated description of the surface dipole might resolve this apparent contradiction.

If we conclude that variations of the surface potential within the Moiré unit cell are not unlikely, then the question arises how large those differences are. To this end we have determined the local barrier height, a quantity that depends directly on the surface potential, in a number of ways. First of all, the effective sample barrier can be obtained from the energies at which the field-emission resonances occur. Using a free-electron description and assuming constant field, Kolesnychenko *et al.* obtained the following equation for the resonance condition:[16]

$$eV_n=\Phi+\left(\frac{3\pi\hbar e}{2\sqrt{2m}}\right)^{2/3}F^{2/3}n^{2/3}. \tag{1}$$

This expression includes the field-emission resonance order $n=1,2,\ldots$, the barrier height Φ, and the electric field F. Fits of the energies to this model are given in Fig. 3. The first field-emission resonance peaks are not considered in the fits. The thus obtained local barriers amount to 3.5, 3.7, and 3.9 eV for the positions labeled with the circle, square, and triangle, respectively.

Alternatively, the local barrier height can be extracted from the exponential dependence of the tunneling current on the tip-sample separation z (Ref. 17),

$$I_t\propto\exp(-2z\sqrt{2m\Phi/\hbar^2}). \tag{2}$$

Φ can be obtained by recording the tunneling current as the tip-sample separation is varied. The acquired curves—typical examples are given in Fig. 5(a)—are fit to Eq. (2), yielding

values of 3.2, 3.4, and 3.5 eV for the locations labeled with circle, triangle, and square, respectively.

According to Eq. (2), the barrier Φ can also be imaged directly by recording the z derivative of the logarithm of the tunneling current, via

$$\Phi = \frac{\hbar^2}{8m}\left(\frac{d \ln I_t}{dz}\right)^2. \quad (3)$$

This is done using a logarithmic and lock-in amplifier by modulating the tip-sample separation z. An image showing $d \ln I_t/dz$, i.e., proportional to $\sqrt{\Phi}$, is given in Fig. 5(c). The contrast in the image shows that there are variations in the barrier height within the Moiré unit cell. Moreover, the $d \ln I_t/dz$ image is inverted with respect to the topography image [Fig. 1(b)], confirming that the regions that first show the field-emission resonance indeed have the lowest barrier. The Φ corrugation that we obtain from $d \ln I_t/dz$ images using Eq. (3) is about a factor of 3 smaller than the values reported earlier. This can be attributed to the fact that the feedback loop is not completely opened during acquisition of the $d \ln I_t/dz$ images. Therefore, the effect of the applied z modulation on the tunneling current can be partially compensated by the feedback system.

Using these different approaches, we have found that the barrier height is likely to differ by several tenths of an eV. To put these values into perspective one can ask what change in the distance d would be required to bring about a change in the local barrier height of about 0.4 eV. Let us consider a very crude electrostatic model to get an idea.

One can approximate the contribution of the polar oxide layer to the surface potential by the electric field caused by a hexagonal array of dipoles with a nearest-neighbor distance of 3.1 Å, that are oriented perpendicularly to the surface. An electron tunneling through this film, experiences the lowest barrier when it traverses the dipole array along the path through the center of the triangle made up by three neighboring dipoles. The field along this path is sketched in Fig. 4 for two different values of the separation d. We have derived an expression that gives the repulsive maximum as a function of the dipole length d. The height of this maximum increases fairly linearly with d for values below 1 Å. Upon extending the size of the dipole lattice, the slope of this linear dependency converges to a value of about 20 eV/Å, if one assumes that the oxide layer is of purely ionic nature (i.e., $q_{\mathrm{Fe}} = -q_{\mathrm{O}} = 2e$). This means that an increase in the distance d of only 0.02 Å would suffice to bring about the required increase in the electrostatic energy of 0.4 eV. In turn, this illustrates that the STM can be very sensitive to geometrical variations within surface structures with a polar termination.

The corrugation of the Moiré pattern that appears in STM images of a thin film of FeO on Pt(111), increases dramatically when the microscope is operated in the field-emission regime. This enhancement can be explained in terms of a variation of the surface potential within the Moiré unit cell. Due to this variation, the local barrier height is not constant and field-emission resonances are observed at different bias voltages. This interpretation is supported by measurements of the local barrier height. Using several methods we find differences on the order of a few tenths of an eV.

We suggest that the variation in the surface potential is caused by the structural inhomogeneity of the FeO thin film. The separation between the Fe and O planes is likely to differ for the different regions within the Moiré unit cell. As a consequence of the polar termination of the surface, modest changes of the Fe-O distance will have a significant effect on the surface dipole.

[1] V. E. Henrich and P. A. Cox, *The Surface Science of Metal Oxides* (Cambridge University Press, Cambridge, UK, 1994).
[2] C. Noguera, *Physics and Chemistry at Oxide Surfaces* (Cambridge University Press, Cambridge, UK, 1996).
[3] A. Barbier *et al.*, Phys. Rev. B **62**, 16056 (2000).
[4] B. Dillmann, F. Rohr, O. Seiferth, G. Klivenyi, M. Bender, K. Homann, I. N. Yakovkin, D. Ehrlich, M. Bäumer, H. Kuhlenbeck, and H.-J. Freund, Faraday Discuss. **105**, 295 (1996).
[5] F. Finocchi *et al.*, Phys. Rev. Lett. **92**, 136101 (2004).
[6] G. H. Vurens *et al.*, Surf. Sci. **201**, 129 (1988).
[7] Y. J. Kim *et al.*, Phys. Rev. B **55**, R13448 (1997).
[8] H. C. Galloway *et al.*, Phys. Rev. B **54**, R11145 (1996).
[9] S. K. Shaikhutdinov *et al.*, Phys. Rev. Lett. **91**, 076102 (2003).
[10] H.-P. Rust *et al.*, Rev. Sci. Instrum. **68**, 129 (1997).
[11] M. Ritter *et al.*, Phys. Rev. B **57**, 7240 (1998).
[12] C. J. Chen, *Introduction to Scanning Tunneling Microscopy* (Oxford University Press, New York, 1993).
[13] R. S. Becker *et al.*, Phys. Rev. Lett. **55**, 987 (1985).
[14] G. Binnig *et al.*, Phys. Rev. Lett. **55**, 991 (1985).
[15] J. Bono and R. H. Good, Surf. Sci. **188**, 153 (1987).
[16] O. Y. Kolesnychenko *et al.*, Physica B **291**, 246 (2000).
[17] G. Binnig and H. Rohrer, Surf. Sci. **126**, 236 (1983).
[18] In addition, the distance between the Fe-O dipole and the polarizable Pt substrate can differ for the various regions as well. A lateral variation in the distance between the FeO dipole and its image dipole will also affect the surface potential.